Giovanelli, C.; Kilkki, O.; Sierla, S.; Seilonen, I.; Vyatkin, V.

Task Allocation Algorithm for Energy Resources Providing Frequency Containment Reserves

Published in:
IEEE Transactions on Industrial Informatics

DOI:
10.1109/TII.2018.2821676

Published: 01/02/2019

Document Version
Peer-reviewed accepted author manuscript, also known as Final accepted manuscript or Post-print

Please cite the original version:
Giovanelli, C., Kilkki, O., Sierla, S., Seilonen, I., & Vyatkin, V. (2019). Task Allocation Algorithm for Energy Resources Providing Frequency Containment Reserves. *IEEE Transactions on Industrial Informatics*, *15*(2), 677-688. Article 8329130. https://doi.org/10.1109/TII.2018.2821676

This is the author's version of an article that has been published in this journal. Changes were made to this version by the publisher prior to publication.
The final version of record is available at http://dx.doi.org/10.1109/TII.2018.2821676

Task Allocation Algorithm for Energy Resources Providing Frequency Containment Reserves

Christian Giovanelli, Olli Kilkki, Seppo Sierla, Ilkka Seilonen, and Valeriy Vyatkin

***Abstract*—The uncertainty caused by the variability in renewable energy production requires the engagement of consumer-side energy production and consumption to provide sufficient flexibility and reliability for the power grid. This study presents an algorithm for allocating tasks to distributed energy resources allowing consumers to provide flexibility for frequency containment reserves. The task allocation algorithm aims at supporting the plug and play of energy resources, and it avoids the need for hard real-time messages during the coordination of the resources. The algorithm combines a novel control strategy with an information and communication technology architecture. The main decision logic of the algorithm is defined together with the distributed control logic. A prototype implementation of the overall system for frequency control is used to evaluate the performance of the algorithm. The simulation results show that the algorithm achieves the specified objectives, and has advantages compared to the state of the art solution.**

***Index Terms*—smart grid, distributed ICT architecture, automated demand response, frequency control, frequency containment reserve, task allocation.**

Nomenclature

C	Set of consumers.
c	Consumer.
R	Set of energy resources.
r	Energy resource.
T	Set of tasks.
τ_1, τ_2	Under/over-frequency task.
t	Time in seconds.
$f(t)$	Frequency.
$\overline{f}(t)$	Filtered frequency.
f_{nom}	Nominal frequency.
Δf_{max}	Maximum frequency deviation.
Δf_{dead}	Dead-band frequency deviation.
$\Delta f(t)$	Frequency deviation.
$\Delta \overline{f}(t)$	Filtered frequency deviation.
β	Time constant.
γ	Time constant.
$DR_{desired}(t)$	Desired control target.
$flex_{target}(\tau, t)$	Target power demand.
$flex(r, \tau, t)$	Power flexibility of an energy resource.
$flex_{total}(\tau, t)$	Total system flexibility.
$flex_{toProvide}(\tau, t, f)$	Flexibility required for one task.
$ta(r, t)$	Task allocation function.
$fa(r, \tau, t)$	Frequency allocation function.
$t_{available}(r, \tau)$	Estimated time of availability of an energy resource.
$b^r(\tau)$	Bidding function of an energy resource for a task
$y(\tau, r)$	Binary function that specifies the allocation of a resource to a task.
$R_{idle}(\tau, t)$	*Idle* function.
$R_{disconnected}(\tau, t)$	*Disconnected* function.
$R_{available}(\tau, t)$	*Available* function.
$R_{allocated}(\tau, t)$	*Allocated* function.
$R_{monitoring}(\tau, t)$	*Monitoring* function.
$R_{reacting}(\tau, t)$	*Reacting* function.
$R_{inoperative}(\tau, t)$	*Inoperative* function.
δ_{total}	Total communication delay.
δ_{cloud}	Cloud-based system communication delay.
δ_{han}	Home area network communication delay.
δ_{min}	Minimum communication delay.
δ_{max}	Maximum communication delay.
ADR	Automated demand response.
EMS	Energy management system.
FCR	Frequency containment reserve.
FCR-N	Frequency containment reserve for normal operation.
ICT	Information and communication technology.
IoT	Internet of Things.
TSO	Transmission system operator.

C. Giovanelli, O. Kilkki, S. Sierla, I. Seilonen, and V. Vyatkin work at the Department of Electrical Engineering and Automation, Aalto University, 02150 Espoo, Finland. E-mail: {firstname}.{lastname}@aalto.fi

V. Vyatkin is also with the SRT, Luleå University of Technology, Sweden, and ITMO University, St. Petersburgh, Russia. E-mail: vyatkin@ieee.org

This research was funded by the Flexible Customer project (285029) of the Academy of Finland.

Manuscript received June 12, 2017; revised XXX.

I. Introduction

In electrical power transmission and distribution systems, the increased penetration of renewable variable energy sources and electric vehicles is entailing major transformations in the power grid. One of these transformations consists of the more widespread use of several ancillary services [1], which aim at ensuring the reliability and stability of the power grid. In fact, in order to guarantee reliability and stability, it is imperative to maintain a constant frequency in the power grid to avoid blackouts and other abnormal situations. If at any time an imbalance occurs in the power grid, i.e. the electricity consumption exceeds the production, the frequency will decrease, and vice-versa. Thus, in order to manage intermittent renewable generation, a mechanism is needed to decrease consumption at times of low generation and increase consumption at times of high generation. This mechanism is called demand response [2], and several market mechanisms for demand response have been developed [3].

One of these ancillary service markets that permits the demand response is the Frequency Containment Reserve (FCR) [4], in which consumers or aggregators offer a certain capacity (in kW), that will be activated automatically in case of a frequency deviation. The aggregators will offer this capacity on an hourly basis on day-ahead or intra-day markets [5]. If the offer is accepted, a load shedding corresponding to this capacity must be activated automatically in case of under-frequency deviation. On the contrary, in case of over-frequency deviation, an additional consumption corresponding to the capacity must be activated.

In order to exploit numerous small energy resources such as household appliances, an aggregator is needed to trade on the FCR markets and to coordinate all of the individual resources. This coordination process can be very dynamic since the state of many resources such as fridges, freezers, boilers or air conditioners is changing dynamically affecting the duration of their availability for demand response actions. With thousands of consumers, a large amount of network traffic over unreliable Internet connections will occur, while FCR imposes hard real-time constraints on the activation of the capacity. Therefore, a solution for FCR exploiting numerous household appliances is a distributed automation problem, in which the control solution is ideally designed together with the ICT architecture. In this study, control and ICT architecture are combined together with the primary objective of developing a task allocation algorithm that employs an auction-based mechanism in order to enable an aggregator to coordinate a set of energy resources to provide reserves for the FCR market. In addition, the task allocation algorithm is designed to achieve the following:

1) avoid the need to send any messages with hard real-time constraints over the public internet, and
2) flexibly handle new resources being plugged in the system as well as existing resources being disconnected.

This paper is structured as follows. Section II presents related work, Section III introduces the system model, followed by the problem formulation in Section IV. Then, Section V proposes distributed algorithms to achieve the objectives 1 and 2. Moreover, Section VI describes the implementation, and Section VII presents simulation results. Section VIII concludes the paper and identifies further work.

II. Related work

The control of frequency controlled reserves for normal operations (FCR-N) is conventionally executed with a droop control in a distributed manner [6], in which generation plants are proportionally adapting their production relative to the power system frequency. Nevertheless, the stability of the electrical grid is threatened by the increase of reserve requirements [7], and the growing penetration of variable renewable generation [8]. Consequently, in order to ensure the stability of the electrical grid, new methodologies for providing the control of FCR-N need to be implemented. Among others, one possible solution is to employ the demand-side to help maintain the balance of the system frequency [9]. In fact, the demand-side could participate in providing the reserve for FCR-N by controlling domestic appliances [10].

Control strategies are required to enable the demand-side to participate in providing the reserve for FCR-N. Different control strategies can be classified according to the communication and coordination requirements that each specific control strategy requires. In fact, a first subset can be composed of uncoordinated control strategies [11], while a second subset includes control strategies that enable the demand-side to be coordinated by a central authority [12], such as an aggregator [13]. The latter control strategies have shown several advantages over the uncoordinated strategies [14]. Among others, the coordination of demand-side allows the aggregator to commit to different amounts of reserves in short time periods. This advantage becomes particularly important when the provided reserves have to be agreed beforehand, i.e., during the planning phases of day-ahead and intra-day markets [5]. However, in order to achieve sufficient capacity to bid on ancillary markets, such as FCR-N, a minimum bid of 0.1MW is required [15], which means that the aggregator must coordinate a large number of distributed domestic appliances. Therefore, the existing work does not consider the resulting ICT and real-time performance challenges or the fact that consumer owned resources should be easy to connect or disconnect from the system without disturbances. Our proposal addresses these aspects with an architecture that divides responsibilities between the aggregator and consumers.

A major scoping decision for any kind of demand response research is the level of detail at which power grid impacts are investigated. There are two bodies of research. Firstly, in several recent works on aggregating numerous loads for demand response purposes [16]–[20], grid impacts such as reactive power and power QoS are not considered. Secondly, few works investigate grid impacts of demand side management in the context of managing several loads [21]–[23], but the case studies are limited to only 16 [22] and 8 [23] loads, respectively; in [21], the loads are not individually simulated. Further [21]–[23] address the problem of voltage control, whereas our research addresses frequency control. Considering the trade-offs related to scalability and the level of detail at which individual loads are simulated on one hand, and investigation of grid impacts on the other hand, we have chosen to focus our investigation to individually simulated loads without investigating grid impacts such as reactive power and power QoS. The reason for this choice is that we propose an aggregator that is able to bid on FCR-N, for which a large number of domestic appliances is required.

The implementation of coordinated control strategies requires the integration of both electrical components and control strategies, with ICT architectures capable of enhancing the performance of the smart grid [24]. This integration will employ middleware architectures, which will be acting as brokers among heterogeneous entities, enabling communication and computation within the future power grid [25]. Recent studies have investigated several solutions of middleware ar-

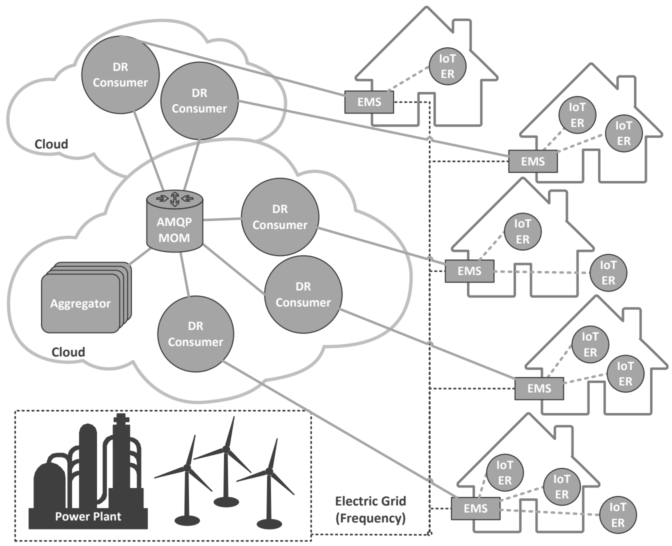

Fig. 1. An overview of the ADR system for frequency control.

chitectures for smart grid [26]. Among others, service-oriented middleware architectures are well motivated by the distributed nature of the problem [27]. So far, however, there has been little research that has combined and integrated ICT architectures for smart grid with control strategies that can execute distributed frequency control. Therefore, this study proposes a comprehensive solution that integrates the ICT architecture with the control strategy enabling the provision of FCR-N reserve with plug-and-play resources.

Task allocation problems have been widely adopted in various engineering domains, including parallel computing [28], data centers [29] and robotics [30]. For example, swarm robotics [31], game-theory [32], and auction-based [33] methods have been applied to enable distributed and heterogeneous entities to cooperate in order to tackle complex tasks. Indeed, the coordination of distributed and heterogeneous energy resources for the provision of FCR reserves consist of a complex task, in which the aggregator has the responsibility of coordinating a large amount of energy resources, as specified in [34]. Therefore, the task allocation algorithm is formulated as a swarm intelligence model as defined by Cornejo et al. [35], where an auction-based mechanism is employed to allocate the tasks to the energy resources [33]. In fact, auctions are multidisciplinary methods employed to solve complex task and resource management problems [36]. Among others, auction-based mechanisms have been extensively studied for multi-robot [37], wireless [38] and parallel computing [39] systems. However, auction mechanisms have not been applied for the allocation of tasks for the participation of consumers owned energy resources to ancillary services in general and FCR-N in particular. Thus, this work is the first attempt to formulate a task allocation algorithm based on an auction mechanism that aims at enabling the participation to the FCR-N reserve provision.

III. System Model

The objective of this study is to develop an algorithm that allows an aggregator to allocate tasks to a set of consumers, defined as C. The algorithm aims at application in an automated demand response (ADR) system that uses the flexibility of the consumers to provide reserve to the FCR-N market. The ADR system is illustrated in Figure 1. The system has a distributed ICT architecture, in which the aggregator communicates with the consumers through a cloud-based system. The communication is performed by means of a message-oriented middleware, which does not guarantee hard real-time performances. Therefore, the aggregator needs to allocate beforehand the tasks for the consumers, in order to avoid the need of sending hard real-time messages over the public Internet. Once allocated with a reaction policy, the consumers need to comply with the policy by controlling locally their Internet of Things (IoT) appliances, and thus providing the required flexibility.

The consumers $c \in C$ participating in FCR-N are provided with an energy management system (EMS), and a set of IoT appliances. The EMS is capable of locally measuring the frequency $f(t)$ of the electric grid by embedding a frequency meter [40], and thus the EMS can locally control the IoT appliances based on $f(t)$ and the tasks allocated by the aggregator. The frequency measurement can be performed with a frequency meter device that satisfies the specifications of the transmission system operator (TSO). For example in Finland, the requirements provided by Fingrid for frequency measurement are that the accuracy of the frequency measurement of the reserve unit shall be at least 10mHz [41]. Since this study focuses on domestic customers, even though the proposed algorithms are generic and equally applicable to single-phase and three-phase appliances, the considered appliances are all single-phase. An appliance is identified as an IoT energy resource ($r \in R$), where R is the set of energy resources in the entire ADR system. The IoT energy resources that can be used by the consumers for the FCR-N consist of power-shiftable appliances (e.g., fridges, freezers, water boilers) or storage appliances (e.g., electric vehicles, batteries). Furthermore, the number $|R|$ of energy resources, utilized for FCR-N in the ADR system, can vary over time.

Define T as the set of tasks that the ADR system needs to execute, and by restricting the scope to frequency control for FCR-N, two tasks ($|T| = 2$) are identified: $\tau_1 \in T$ and $\tau_2 \in T$, which respectively represent the under-frequency and the over-frequency reaction of the ADR system. In addition, given $t \in \mathbb{R}_{\geq 0}$, representing the discrete time in seconds, it is possible to define the following functions:

- $flex_{target}(\tau, t)$ consists of the target power demand for a task τ at the given time t. This function represents the amount of committed reserves that the ADR system needs to provide.
- $flex(r, \tau, t)$ specifies the flexibility, in terms of power, that an energy resource $r \in R$ of a consumer $c \in C$ can supply to the task $\tau \in T$, at a given time t.
- $flex_{total}(\tau, t)$ refers to the total flexibility provided by

This is the author's version of an article that has been published in this journal. Changes were made to this version by the publisher prior to publication.
The final version of record is available at http://dx.doi.org/10.1109/TII.2018.2821676

the energy resources R of the ADR system to a task τ:

$$flex_{total}(\tau, t) = \sum_{r \in R} flex(r, \tau, t) \tag{1}$$

To participate in the FCR-N market, the aggregator needs to coordinate the energy resources R in order to satisfy the requirements imposed by the TSO. The TSO requires that the provided reserve must be available and fully activated within three minutes after a frequency deviation (Δf_{max}) of +/- 0.1 Hz from the nominal frequency (f_{nom}) of 50 Hz. In addition, the TSO defines a maximum dead-band deviation (Δf_{dead}) of +/- 0.02 Hz, in which the reserves are not required to react. The amount of provided reserve is the activated power after three minutes against the step change. In this study, the minimum power reserve size of 0.1 MW, required by the TSO for the participation to the FCR-N market [15], is not considered.

The TSO compensates the aggregator for offering a load to FCR-N, so the aggregator will share benefits with users. FCR-N is an hourly market with high price variations, and the aggregator is required to bid on the day before. If users have specific expectations for their financial compensation, the bid can be set high enough to ensure that the aggregator can profitably meet these expectations.

IV. Problem Formulation

The consumers are required to react to deviations $\Delta f(t)$ from the nominal frequency f_{nom}. However, instantaneous reaction to any abrupt changes in the frequency or errors in its measurement could lead to unwanted oscillations in the control and in the realized frequency of the grid. Therefore, we target a first-order filtered control signal, by computing a filtered value

$$\overline{f}(t+1) = e^{-\frac{1}{\beta}}\ \overline{f}(t) + (1 - e^{-\frac{1}{\beta}})f(t) \tag{2}$$

for the frequency deviation, with a time constant of β. The time constant is chosen with $\beta = \frac{-\gamma}{log(1-p)}$, such that the control satisfies the requirements of the TSO, of reaching e.g. $p = 99\%$ of the required activation time γ, which value was chosen to be 120 seconds to fulfill the requirement to activate the reserve within three minutes ($\gamma < 180$) [15].

Based on the filtered frequency, we can define a desired control target

$$DR_{desired}(t) = \begin{cases} (4) & |\Delta f_{dead}| < \left|\Delta \overline{f}(t)\right| < |\Delta f_{max}| \\ 0 & \left|\Delta \overline{f}(t)\right| < |\Delta f_{dead}| \\ (5) & \left|\Delta \overline{f}(t)\right| > |\Delta f_{max}| \end{cases} \tag{3}$$

where function (4) is defined as:

$$sign(\Delta\overline{f}(t))\ (\left|\Delta\overline{f}(t)\right| - \Delta f_{dead})\ \frac{flex_{target}(\tau, t)}{(\Delta f_{max} - \Delta f_{dead})} \tag{4}$$

and function (5) is:

$$sign(\Delta\overline{f}(t))\ flex_{target}(\tau, t) \tag{5}$$

The amount of reserve that the ADR system needs to provide is required to scale linearly with the frequency deviation Δf from f_{nom}. Therefore, the aggregator has an objective

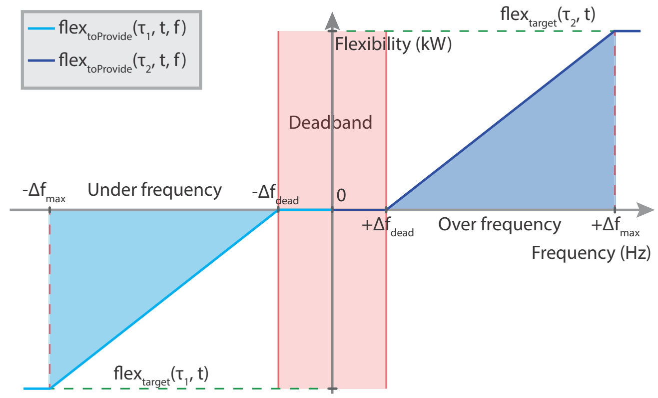

Fig. 2. The objective function $flex_{toProvide}(\tau, t, f)$ and the target reserve function $flex_{target}(\tau, t)$ for both the under-frequency and the over-frequency tasks.

function $flex_{toProvide}(\tau, t, f)$, which represents the flexibility required for a task τ at given time t giving the frequency value f. Figure 2 shows how the function is defined for both cases: the under-frequency $flex_{toProvide}(\tau_1, t, f)$, and the over-frequency $flex_{toProvide}(\tau_2, t, f)$ containment.

The aggregator needs to allocate the required flexibility for both τ_1 and τ_2 at any given time t. For this reason, the total flexibility that the ADR system can provide for a task τ will always have to exceed the target power demand for τ at any given time t. Therefore, if the following condition subsists for every t:

$$flex_{target}(\tau, t) - flex_{total}(\tau, t) < 0 \tag{6}$$

then the task allocation problem is satisfiable. This equation requires the aggregator to estimate ahead the hourly $flex_{target}(\tau, t)$ that the ADR system will be able to supply to the FCR-N market, enabling the ADR system to provide the reserve for the entire hour, and thus fulfilling the participation requirements. Since the estimation of the $flex_{target}(\tau, t)$ is not a part of the scope of this study, it is assumed that the aggregator will solve task allocation problems in which the equation (6) is always satisfied.

V. Proposed Algorithm

The task allocation algorithm is executed by the aggregator, and it aims at dynamically allocating tasks to the energy resources of the consumers, enabling their participation in the FCR-N. Then, the consumers are required to adhere to the given tasks, and thus provide the flexibility to the power grid. According to [42], key data required by the TSO for the validation of the FCR-N application include the active power and the grid frequency measurements which should behave according to Figure 2. A detailed investigation on reactive power and other power QoS information is not included but could be investigated in further work involving more detailed controller design and simulations of the power system. The focus of the present work is on the level of the aggregator and on the problem of allocating large numbers of small consumer owned loads.

A. Energy Resource Operational States

The energy resources R of the ADR system consist of IoT devices which are controllable by the EMS of the consumers in order to provide flexibility to the grid. Based on the task allocation algorithm, at any given time t an energy resource can be either allocated to one task τ or none. Therefore, a task allocation function ta is defined, which assigns for the time t either one or zero tasks for each energy resource r:

$$ta(r,t) : R \times \mathbb{R}_{\geq 0} \rightarrow T \cup \{\varnothing\} \tag{7}$$

Since resources can simultaneously participate in several tasks, such as τ_1 and τ_2, the idle function is defined in terms of specific tasks as follows:

$$R_{idle}\left(\tau_j, t\right) = \{r \in R : ta(r,t) = \varnothing \vee ta(r,t) = \tau_i (i \neq j)\} \tag{8}$$

Each energy resource that belongs to $R_{Idle}(\tau, t)$ is in the *Idle* state. On the other hand, the energy resources that are allocated to τ belong to the *Allocated* state, and the set of these energy resources $R_{allocated}(\tau, t)$ can be specified as:

$$R_{allocated}\left(\tau, t\right) = \{r \in R : ta(r,t) = \tau\} \tag{9}$$

Figure 3 presents the *Idle* and the *Allocated* states as composite states for the energy resources, in which the control logic is defined as a state machine.

Each energy resource of the ADR system can belong to the *Idle* composite state for two distinct reasons. Firstly, because of the inability of the energy resource to provide the flexibility to the task τ. Thus, the energy resources are disconnected from the ADR system for FCR-N. In this case, the energy resource belongs to the *Disconnected* state:

$$\begin{aligned} R_{disconnected}\left(\tau, t\right) = R_{idle}\left(\tau, t\right) \cap \\ \{r \in R : flex(r, \tau, t) = 0\} \end{aligned} \tag{10}$$

Secondly, the *Available* state is defined for the energy resources that can provide flexibility to τ, but they have not been allocated to the task. Therefore, the *Available* state is specified as:

$$R_{available}\left(\tau, t\right) = R_{idle}\left(\tau, t\right) \cap \{r \in R : flex(r, \tau, t) > 0\} \tag{11}$$

Depending on the capability of an energy resource to provide flexibility to τ, a consumer can locally change the state of the energy resource between the two states: *Disconnected* and *Available*. At each change of state, the consumer needs to notify the aggregator through the message-oriented middleware, as detailed in [43]. If an energy resource is moved to the *Available* state, the consumer sends a bid to the aggregator containing the flexibility value (i.e. $flex(r, \tau, t) > 0$) and the estimated time for which the energy resource will be *Available*, defined as $t_{available}(r, \tau)$. Whereupon, the energy resource is considered as being plugged to the ADR system for providing flexibility to τ. On the other hand, when the energy resource changes to the *Disconnected* state, it is unplugged, and thus not considered for τ. In this case, the consumer needs to notify the aggregator, thus canceling the previous bid of the energy resource r for the task τ, indicating that $flex(r, \tau, t) = 0$.

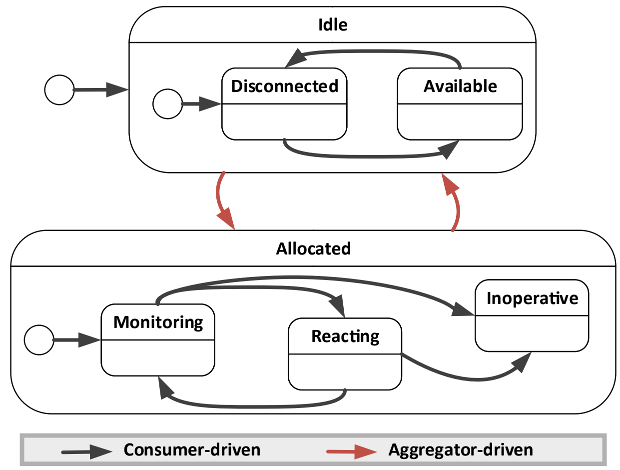

Fig. 3. The operational states of the IoT energy resources. The *Idle* composite state represents the energy resources that are either *Disconnected* from the ADR system or *Available* to participate in FCR. The *Allocated* composite state represents all the energy resources that have been allocated to provide the reserve, which are either *Monitoring* the frequency without reacting, *Reacting* to the frequency deviations, or *Inoperative*, and thus waiting to be replaced and deallocated by the aggregator.

The composite state *Allocated* is composed of the energy resources that have been allocated by the aggregator to perform the task $\tau \in T$. The energy resources in this composite state can be one of three different states: the *Monitoring* state ($R_{monitoring}$), the *Reacting* state ($R_{reacting}$), and the *Inoperative* state ($R_{inoperative}$). The set of energy resources in the *Monitoring* state consists of the resources $r \in R$ that can provide flexibility to the power grid. These resources are currently not reacting to the frequency deviations, since their allocated frequency deviation $\Delta f_{alloc}(r)$ is not exceeded by filtered deviation $\Delta \overline{f}(t)$:

$$\begin{aligned} R_{monitoring}\left(\tau, t\right) = R_{allocated}\left(\tau, t\right) \cap \\ \{r \in R : flex(r, \tau, t) > 0 \wedge \Delta \overline{f}(t) < \Delta f_{alloc}(r)\} \end{aligned} \tag{12}$$

The energy resources that are currently reacting to a frequency deviation are in the *Reacting* state, which is defined as:

$$\begin{aligned} R_{reacting}\left(\tau, t\right) = R_{allocated}\left(\tau, t\right) \cap \\ \{r \in R : flex(r, \tau, t) > 0 \wedge \Delta \overline{f}(t) \geq \Delta f_{alloc}(r)\} \end{aligned} \tag{13}$$

The final state is called *Inoperative*. The *Inoperative* state consists of each energy resource that can no longer provide any flexibility to the power grid. These energy resources are waiting to be deallocated to the *Idle* state by the aggregator, which should then replace their share in the flexibility provided with other energy resources that are in the *Available* state. Hence, the set $R_{inoperative}$ of energy resources that belongs to the *Inoperative* state can be defined as follows:

$$\begin{aligned} R_{inoperative}\left(\tau, t\right) = R_{allocated}\left(\tau, t\right) \cap \\ \{r \in R : flex(r, \tau, t) = 0\} \end{aligned} \tag{14}$$

B. Frequency Task Allocation Algorithm

By executing the frequency task allocation algorithm, the aggregator aims at allocating the required flexibility to each of the given tasks. The objective of the algorithm is to allocate the flexibility of the energy resources in such a way that the reserve provided by the ADR system remains as close as possible to the objective function $flex_{toProvide}(\tau, t, f)$. The frequency task allocation algorithm is composed of three main procedures: the frequency task allocation, the continuous allocation, and the corrective control.

1) Frequency task allocation procedure: this represents a total reallocation of the flexibility provided to a task τ. The procedure is executed once every 15 minutes, and it can be formulated as a multi-task (τ_1 and τ_2), multi-resource ($r \in R$) and multi-unit auction, where one unit corresponds to one Watt and one energy resource can provide multiple units. Further, $flex_{target}(\tau, t)$ represents the total amount of units for one task τ. The consumers, in order to make an energy resource *Available*, send a bid to the aggregator which express the flexibility that the energy resource can provide ($flex(r, \tau, t)$) and the expected time of availability ($t_{available}(r, \tau)$) of the energy resource for the task τ. Once received a bid, the aggregator calculates a bid function $b^r(\tau)$ as follows:

$$b^r(\tau) = flex(r, \tau, t) \cdot t_{available}(r, \tau) \tag{15}$$

In addition, the aggregator defines the function $y(\tau, r)$, which specifies whether a resource is allocated or not to the task τ:

$$y(\tau, r) = \begin{cases} 1 & \text{if } r \textit{ allocated to } \tau \\ 0 & \text{if } r \textit{ not allocated to } \tau \end{cases} \tag{16}$$

Thus, the frequency task allocation procedure can be formulated as an auction-based problem in which we minimize the amount of resources allocated to the task τ, in respect to the bid functions $b^r(\tau)$ as:

$$\min_{y(\tau,r)} \sum_{r \in R_{available}} \sum_{\tau \in T} b^r(\tau) y(\tau, r) \tag{17}$$

s.t.

$$\sum_{\tau \in T} \sum_{r \in R_{available}} flex(r, \tau, t) \cdot y(\tau, r) - flex_{target}(\tau, t) \geq 0 \tag{18}$$

$$\sum_{\tau \in T} y(\tau, r) \leq 1, \forall r \in R \tag{19}$$

$$y(\tau, r) = 0, 1, \forall \tau \in T, \forall r \in R \tag{20}$$

where (18) expresses the objective to provide the target flexibility ($flex_{target}(\tau, t)$) required when the deviation from f_{nom} is the maximum specified by the FCR-N (i.e. Δf_{max}); while (19) specifies the condition that each energy resource can be allocated to a single task τ at a time.

Having selected the best energy resources from the $R_{available}$, the aggregator needs to define the frequency deviation Δf_{alloc} at which each energy resource needs to react, thus providing its flexibility. Hence, the selected energy resources are randomly ordered, allowing the random allocation the Δf_{alloc} to each energy resource, and thus avoiding the most frequent exploitation of few better resources when the frequency deviations are smaller. Then, the frequency deviation $\Delta f_{alloc}(r)$ is calculated by the frequency allocation function $fa(r, \tau, t)$. For each resource r allocated to τ by $y(\tau, r)$, the function $fa(r, \tau, t)$ derives the respective frequency deviations ($\Delta f_{alloc}(r)$) in order to provide a linear behavior as the objective function $flex_{toProvide}(\tau, t, f)$. Figure 4 shows in detail how the frequency deviations $\Delta f_{alloc}(r)$ are allocated by the frequency task allocation procedure. Once every $\Delta f_{alloc}(r)$ is calculated for each selected resource r, the aggregator proceeds in allocating the energy resources by sending an allocation message, where the allocated task τ and $\Delta f_{alloc}(r)$ are specified. Consequently, this operation moves the energy resource from the *Idle* state to the *Allocated* state.

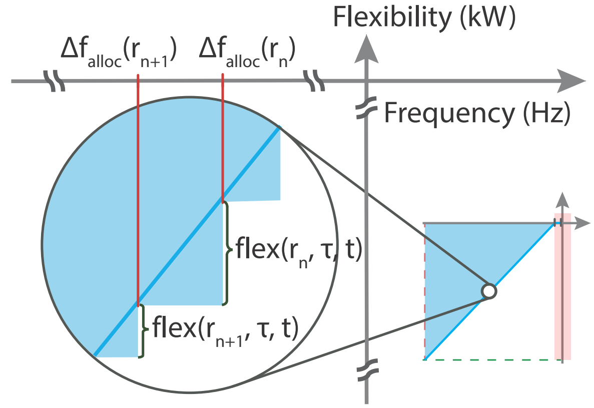

Fig. 4. The allocation of the energy resources performed by the frequency task allocation procedure. The flexibility $flex(r_{next}, \tau_1, t)$ of the *Available* energy resources are collected in sequence and each resource is allocated with a reaction policy that specifies the respective frequency deviation $\Delta f_{alloc}(r_{next})$.

The *frequency task allocation procedure* enables the readjustment of the flexibility provided by the ADR system in order to adhere to the objective function $flex_{toProvide}(\tau, t, f)$, as shown in Figure 2. Moreover, the frequency task allocation procedure, in conjunction with the following procedure named *continuous allocation procedure*, enables the plug and play of energy resources.

2) Continuous allocation procedure: while the frequency task allocation procedure is executed at pre-defined time intervals, the continuous allocation procedure runs continuously to replace inoperative energy resources. The continuous allocation procedure replaces the energy resources that are in the *Inoperative* state with new energy resources $r \in R_{available}$. The algorithm monitors if there are energy resources in the $R_{inoperative}$ set, and when it finds any, it starts deallocating each of the energy resources $r_{dealloc} \in R_{inoperative}$. Then, the aggregator retrieves energy resources $r \in R_{available}$ in order to replace the flexibility that was previously guaranteed by $r_{dealloc}$. The replacement of an *Inoperative* energy resource ($r_{dealloc}$) is performed in a similar way of the frequency task allocation procedure (i.e. (15) - (20)), in which only the single task where the $r_{dealloc}$ was allocated is considered, and denoted as $\tau_i \in T$ (i.e. τ_1 or τ_2). The only change in the formulation is in (18), which is modified in order to replace only the flexibility of the $r_{dealloc}$, and defined as:

$$\sum_{r \in R_{available}} flex(r, \tau_i, t) \cdot y(\tau_i, r) - flex(r_{dealloc}, \tau_i, t) \geq 0 \tag{21}$$

3) Corrective control: the requirements for an intelligent load that provides ancillary services on the FCR-N market are specified as relative changes to a baseline consumption that is assumed to be constant. The thermodynamic energy resources considered in this paper do not have a constant baseline consumption, so it is problematic to validate that the system fulfills this specification. Hence, the purpose of the corrective control is to coordinate a subset of energy resources in such a way as to achieve this constant baseline consumption. Thus, the flexible resources from a subset of the consumers are reserved for the purpose of this corrective control instead of being used for reacting to frequency deviations. The consumption of these consumers is increased if the total consumption of all the consumers in the system is less than the baseline; similarly the consumption of these consumers participating in the corrective control is decreased if the total consumption of all consumers exceeds the baseline. The corrective control is run by the aggregator at regular intervals; an interval of 30s was used to obtain the results in this paper. The corrective control may command the refrigerators of individual consumers to switch on or off, making sure that the comfort boundaries in Figure 5 are not violated.

C. Energy Resource Control Logic

As shown in Figure 3, the aggregator, by allocating and deallocating the energy resources, is driving each change of state between the two composite states (*Allocated* and *Idle*) of the energy resources, while the internal transitions within each composite state are locally controlled by the consumers EMS. The clear division of responsibilities between the aggregator and consumers allows the ADR system to avoid the need of real-time messages. In fact, once the aggregator allocates preemptively the task τ with the respective frequency deviation $\Delta f_{alloc}(r)$ to an energy resource, the energy resource moves in the *Allocated* composite state. Then, within the *Allocated* state, the consumers need to control the energy resource autonomously in order to react locally to the frequency changes by following a specified control logic.

Algorithm 1 Energy Resources Control Logic

function IoTERControlLogic
  while $ta(r,t) = \tau_1$ **do**
    while $flex(r,\tau_1,t) > 0$ **do**
      if $\Delta\overline{f}(t) \geq \Delta f_{alloc}(r) \wedge$
        $stateOf(r) = Monitoring$ **then**
          $stateOf(r) = Reacting;$
      else if $\Delta\overline{f}(t) < \Delta f_{alloc}(r) \wedge$
        $stateOf(r) = Reacting$ **then**
          $stateOf(r) = Monitoring;$
    $stateOf(r) = Inoperative;$

A control logic example for task τ_1 of an energy resource r is presented in Algorithm 1. The algorithm defines how an EMS should control an energy resource that has been allocated by the aggregator to provide FCR-N. As long as the energy resource is allocated to τ_1, and it can provide flexibility to the ADR system, the EMS maintains the energy resource either in the *Monitoring* or *Reacting* states. Indeed, when the filtered frequency deviation $\Delta\overline{f}(t)$ results to be greater than the allocated frequency deviation $\Delta f_{alloc}(r)$, then the EMS places the energy resource into the *Reacting* state, and by controlling the energy resource it provides the promised flexibility $flex(r,\tau_1,t)$. On the contrary, if $\Delta\overline{f}(t)$ is less than Δf_{alloc}, the energy resource will be placed in the *Monitoring* state. Moreover, if the energy resource is not deallocated by the aggregator before it can no longer provide flexibility, the EMS drives the energy resource into the *Inoperative* state, and communicates this to the aggregator, which will replace the resource as soon as possible.

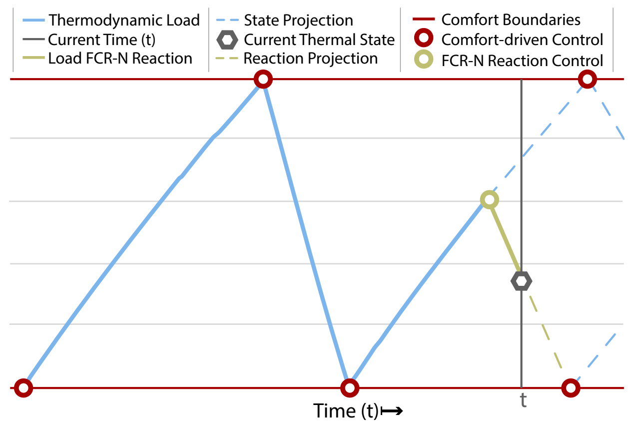

Fig. 5. Example of the control applied to a thermodynamic energy resource in order to provide FCR-N reserves while maintaining the comfort constraints.

Besides the control logic utilized by the EMS to provide flexibility for FCR-N, a comfort-driven control is implemented for the energy resources. This control is intended to maintain the appliance within the comfort limits, which according to the type of energy resources can be either embedded in the appliances or defined by the users. The user comfort is prioritized over the participation in the FCR containment, therefore the EMS gives the priority to the latter control over the energy resource control logic defined in Algorithm 1.

Figure 5 presents the state dynamics of a thermodynamic energy resource, where the control logic for providing FCR-N reserves and the comfort-driven control are combined. The comfort-driven control is executed every time the energy resource reaches its comfort boundaries, and it has the priority over the provision of reserves. When the boundaries are reached while the energy resource is reacting to the frequency deviations, the flexibility of the thermal energy resource becomes equal to zero ($flex(r,\tau,t) = 0$), driving the energy resource into the *Inoperative* state, and the energy resource is then replaced by the *continuous allocation procedure*.

VI. Implementation

The ADR system has been implemented as a prototype ICT system composed of several applications, developed in Java. The first application operates as the aggregator, and contains the frequency task allocation algorithm. The second application implements a scalable number of consumers, in which an EMS and a set of IoT resources for FCR-N are

This is the author's version of an article that has been published in this journal. Changes were made to this version by the publisher prior to publication.
The final version of record is available at http://dx.doi.org/10.1109/TII.2018.2821676

modeled for each consumer. The EMS operates as a gateway between the IoT resources of the consumer's household and the cloud-based system of the ADR system. The modeled population of energy resources consist of refrigerators, which have been implemented according to [44]. The refrigerators are initialized with random values, and their dynamics are simulated for twelve hours with the comfort-driven control, before being utilized for the ADR system simulations. In addition, the refrigerators have been modeled with a minimum resting period, which is uniformly distributed between the range of 2 and 4 minutes. Finally, a third application outputs the frequency dynamics $f(t)$ of the ADR system.

The communication between the aggregator and the consumers was performed through RabbitMQ [45], a message-oriented middleware that implements the Advanced Message Queuing Protocol (AMQP) [46]. The communication logic was designed in order to exploit several advantages of AMQP, such as the advanced routing of messaging as well as both publish-subscribe and point-to-point request-response communication, as shown in [43].

Time-varying communication delays have been included in the simulations of the ADR system. The delays were considered as end-to-end, from the aggregator to the IoT energy resources, passing through the EMSs of the consumers. Along the end-to-end path, the total delay δ_{total} was considered as the sum of the communication delay of the cloud-based system δ_{cloud} [47] and the delay in the consumers' home area network δ_{han} [48], as follows:

$$\delta_{total} = \delta_{cloud} + \delta_{han} \tag{22}$$

in which δ_{cloud} and δ_{han} are both defined as:

$$\delta_{cloud} = \delta_{han} = \delta_{min} + rand(0, \delta_{max}) \tag{23}$$

where δ_{min} is the minimum delay, δ_{max} is the maximum delay and $rand(0, \delta_{max})$ generates a random number within the interval $[0, \delta_{max}]$. In order to inject both the delays in the ADR system, the communication between the energy resources and the EMSs has been modeled in such a way to allow δ_{han} to be added, while for the cloud-based system the delay was injected in the AMQP communication through a plug-in called RabbitMQ Delayed Message Plugin [49].

A population of 5000 IoT energy resources was utilized for the simulations. For this population, the required $flex_{target}(\tau_1, t)$ was arbitrarily chosen to be 50 kW for both tasks of the aggregator, the under-frequency τ_1 and the over-frequency τ_2. Since the controlled power was relatively small, it was assumed that the controlled power was not altering the frequency dynamics of the ADR system. The frequency dynamics $f(t)$ were modeled with real frequency measurement data, which were taken from the historical frequency measurement data of the Nordic power system provided by Fingrid [50]. Moreover, the specified dead-band deviation Δf_{dead} was 0.02 Hz, while the maximum deviation Δf_{max} considered was 0.1 Hz, as required by FCR-N.

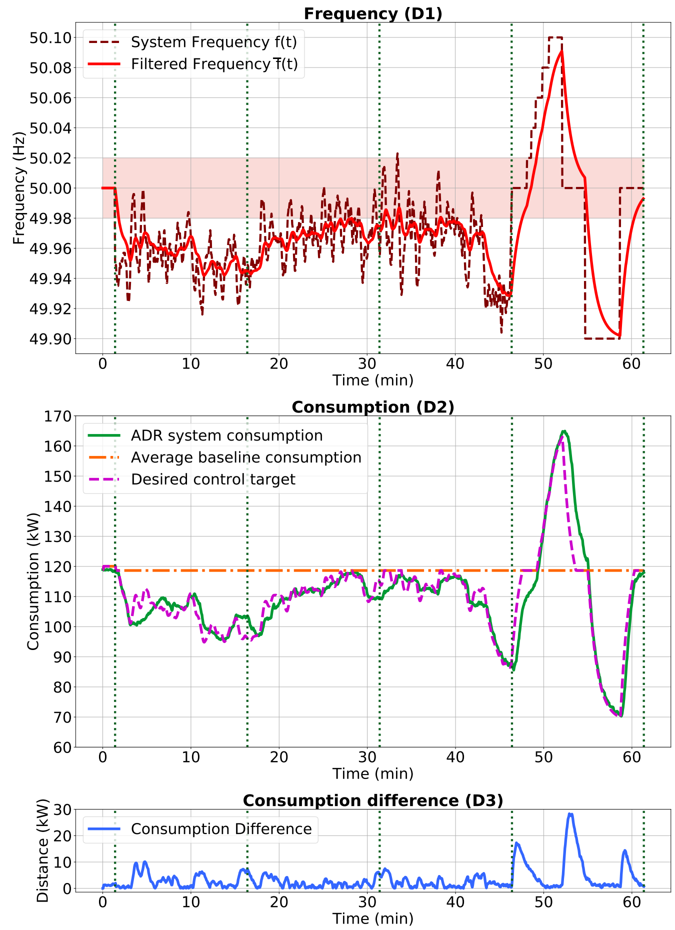

Fig. 6. (D1) The frequency $f(t)$ injected to the ADR system using real frequency data from Fingrid [50] and custom frequency patterns, and the filtered frequency $\overline{f}(t)$. (D2) The realized consumption of the ADR system compared with the $DR_{desired}(t)$. (D3) The difference between the realized consumption of the ADR system and the $DR_{desired}(t)$. Moreover, the vertical dotted lines represent the time when the frequency task allocation procedure was executed by the aggregator.

VII. Simulation Results

A. Performance of proposed solution

The first simulation was used to analyze the performance of the ADR system. The simulation aimed at comparing the actual reaction control of the system with the $DR_{desired}(t)$ specified in (3), and at identifying the possible pitfalls for the ADR system. Thus, one hour simulation was executed, in which in the first 45 minutes real data from Fingrid [50] were injected into the system, while, for the remaining time, customized frequency data were utilized (Figure 6.D1). In addition, the total end-to-end delay δ_{total} was distributed between a minimum of one to a maximum of three-second. Thus, the results obtained from the simulation are presented in Figure 6.D2, which represents the ADR system consumption. Based on the reactions during the last 15 minutes of the simulation, it is possible to observe that during the constant frequency deviations of Δf_{max} for a long time period (starting at the minute 54) the reactions of the energy resources are well aligned with the desired control target $DR_{desired}(t)$. However, with a shorter frequency deviation based incremental

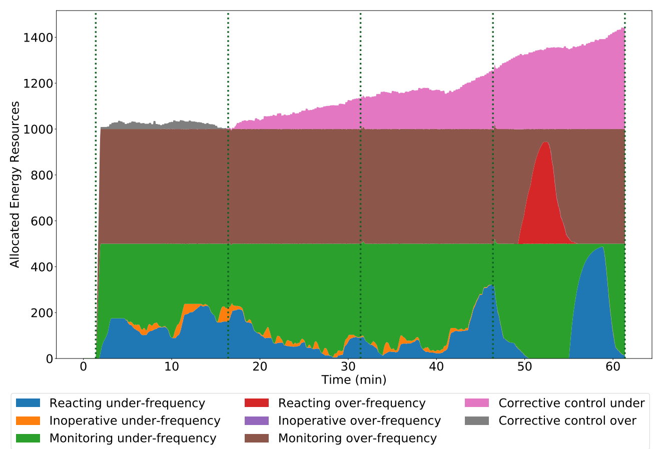

Fig. 7. The energy resources allocated to the *Allocated* composite state over time for the under-frequency and the over-frequency cases, and the amount of energy resources used by the corrective control in one hour simulation.

steps, as in the over-frequency deviation (starting at the minute 48) of the simulation, while the reaction remains aligned with $DR_{desired}(t)$, during the *counter-reaction* (i.e. when the frequency deviation restores within Δf_{dead}) the actual reaction of the system has a delay, which results in a large difference between the desired control target $DR_{desired}(t)$ and the realized consumption of the ADR system (Figure 6.D3). A similar behavior can be observed during the first 45 minutes of the simulation with real frequency data, in which delays occur during the counter-reaction phase. Since the delays were only observed in the counter-reaction phase, the result shows that the delays are caused by the resting period of the devices, rather than from the possible communication delays of the ICT system and the task allocation algorithm. Thus, the resting period of the devices is the cause of the observed peaks in the consumption difference between the desired control target $DR_{desired}(t)$ and the realized consumption of the ADR system (Figure 6.D3).

Another important aspect, presented in Figure 6.D1, is the comparison between the real frequency data $f(t)$, and the relative filtered frequency $\Delta\overline{f}(t)$. As can be seen, the frequency of the Nordic power system is affected by frequent fluctuations. This characteristic motivates the choice of filtering the frequency in order to avoid oscillations in the realized frequency of the grid, caused by erroneous reactions of the consumers in the DR. In addition, Figure 6.D2 shows how the aggregator, within the hour of simulation, tries to apply the corrective control in the ADR system in order to maintain the total consumption of the system (when the frequency is within the dead-band) to a certain value established at the beginning of the hour. In fact, all the decentralized reactions to the frequency are then shaping the total consumption relatively to the established consumption value.

Figure 7 shows the amount of energy resources in the ADR system that have been in the *Allocated* composite state during the first simulation, for both tasks, τ_1 and τ_2. In addition the diagram shows the amount of energy resource utilized by the corrective control during the simulated hour. It is possible to observe that the energy resources allocated for the task τ_1 were actively participating to the frequency control and thus providing reserve to the grid. The diagram shows how the energy resources were changing between the three states of the *Allocated* composite state, based on the filtered frequency $\Delta\overline{f}(t)$. Important to notice are the small accumulations of *Inoperative* energy resources during the under-frequency reaction, which typically occur during a counter-reaction phase. This phenomenon is caused by the resting period of the refrigerators, that does not permit the energy resources to react instantaneously at two consecutive frequency drops, hence requiring the reschedule the energy resources. Therefore, a combination of different devices, with (e.g. refrigerators) and without (e.g. HVAC) resting period, would mitigate the accumulation of *Inoperative* energy resources during the counter-reaction phase. Moreover, the diagram shows also the amount of energy resources controlled by the corrective control. During the simulated hour, the amount of energy resources utilized by the corrective control is growing, due to the large participation in the frequency control for the under-frequency task that causes the demand of the ADR system to be shifted.

A second simulation was executed in order to verify the impact of the communication delays on the ADR system. For this second simulation, the frequency measurements, injected into the ADR system, were taken from the Continental Europe [51], demonstrating that the developed system can be operational in other regions with different frequency characteristics (Figure 8.D1). The performance of the ADR system with different communication delays are shown in Figure 8 (D2, D3, D4). As can be seen, the ADR system has similar performance regardless the distribution of the total communication delay δ_{total}, which was randomly distributed in the intervals [1,3], [10,30], and [30,90] seconds. This demonstrated that the ADR system is robust to the communication delays, and does not require real-time communication for the participation to the FCR-N.

In the worst case scenario of Figure 8, delays were distributed in the range [30,90]. These values were determined experimentally, since with a higher value significant performance degradation was observed. Thus, the significance of these results is to demonstrate that the system is robust against delays that are longer than what can be expected in the public internet. The Continuous Allocation Procedure is executed every 3s. In this procedure, *Inoperative* resources are deallocated and replaced. As explained in Figure 3, the aggregator immediately moves a resource away from the *Inoperative* state, so the percentage of *Inoperative* resources will remain minor as long as the communication delays are within certain limits. Due to the fact that *Inoperative* resources represent a minor fraction of the total resources, delays in their replacement will similarly have minor impact on overall performance as observed in Figure 8. Quantitative values for ‘minor’ and ‘within certain limits’ have been determined experimentally. As stated above, the communication delays were distributed in the range [30,90] in the worst case scenario for which the system has been simulated. In this case, the ‘minor’ fraction of *Inoperative* resources is presented in Figure 9.

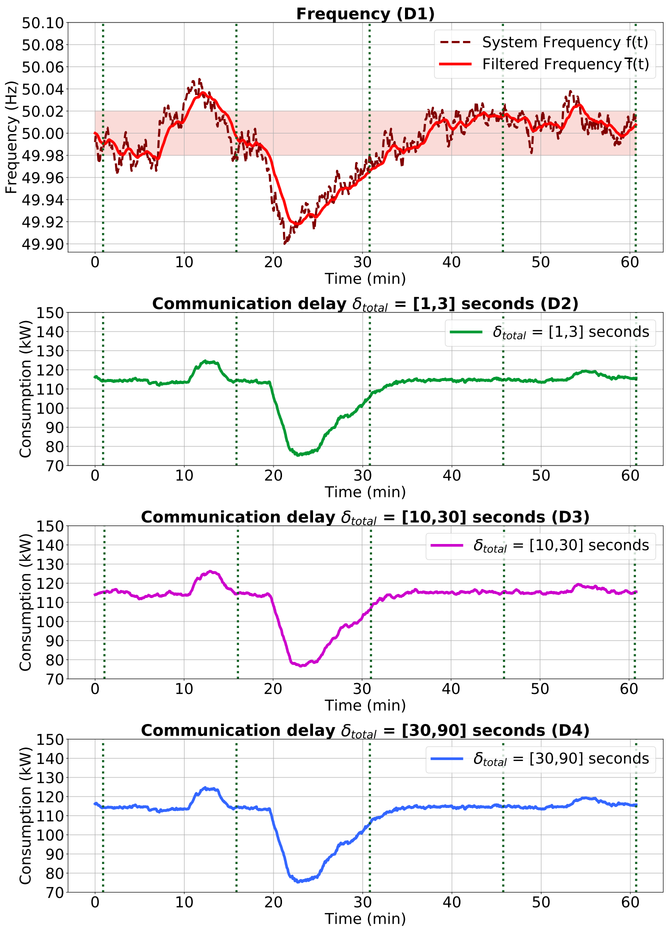

Fig. 8. (D1) The frequency $f(t)$ injected to the ADR system using real frequency data from the Continental Europe [51]. (D2) The realized consumption of the ADR system with a δ_{total} within the range [1,3] seconds. (D3) The realized consumption of the ADR system with a δ_{total} within the range [10,30] seconds. (D4) The realized consumption of the ADR system with a δ_{total} in the range [30,90] seconds.

B. Comparison with the State of the Art

The objective of the third simulation was to compare the presented task allocation algorithm with the decentralized solution of frequency control presented in [11], in which the energy resources are reacting in a totally decentralized DR system, with no communication required, and the consumers are reacting directly to the frequency deviations based on a frequency-time characteristic which defines when the energy resource should provide the flexibility. Whilst this solution does not require any cooperation, one limitation is the static definition of the frequency-time characteristic that the energy resources need to follow, without enabling the plug and play or the disconnection of the energy resources. Thus, there is no automatic control that compensates for a resource that is unexpectedly plugged out of the ADR system. In fact, such automatic control is needed to ensure that the ADR system is able to provide the targeted power $flex_{target}(\tau, t)$, which was sold by the aggregator to the ancillary market.

A second disadvantage is the incapability of the totally decentralized solution to have control on the amount of reserve effectively provided to the grid. Figure 10.D2 shows the consumption profiles for one hour simulation of the task allocation algorithm and the decentralized solution. By comparing the first period (15 minutes) of simulation with the last 2 periods (30 minutes), despite having similar frequency deviations in the ADR system it can be seen that in the first period the two systems have similar responses and in the last two periods the two solutions provide different responses in terms of total consumption. This anomaly is due to the fact that after a short time the static allocation starts to lose its capability to provide the reserves, and, even if the energy resources are still reacting to the frequency deviations, the total consumption of the static solution rapidly increases. On the other hand, the task allocation algorithm allocates the energy resources and applies the corrective control based on a total consumption value of the ADR system (i.e. 120 kW for the executed simulation) established at the beginning of every hour. This solution enables the control of the provided reserves during each hour, by dynamically allocating resources and utilizing a mixed control strategy: decentralized, by allocating the tasks, combined with centralized, by applying the corrective control.

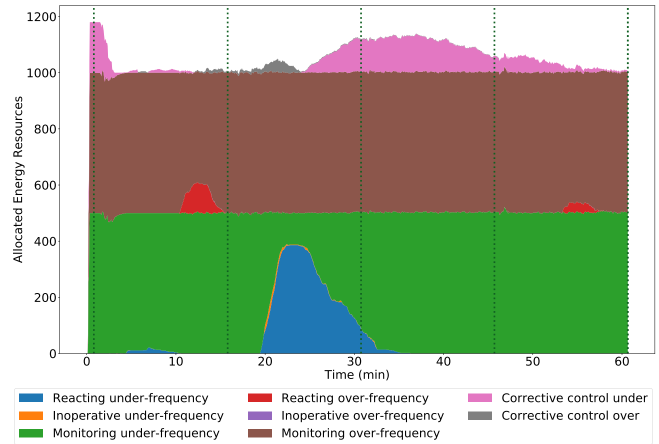

Fig. 9. The energy resources allocated to the *Allocated* composite state in the worst case scenario (D4) of Figure 8, where the δ_{total} was in the range [30,90] seconds.

VIII. Conclusion

The aim of the present research was to design a task allocation algorithm for frequency control, in which the control solution was combined with the ICT architecture. While this work does not aim at providing a fundamental contribution to the task allocation state of the art, it is the first attempt to apply a task allocation algorithm to the demand response of consumer owned loads, and more specifically to the participation of energy resources to ancillary service markets, such as the FCR-N market. The main objectives of the allocation algorithm were to avoid the need of hard real-time messages for the coordination of the energy resources, and to support the plug in and disconnection of the energy resources. Based on these objectives, the proposed task allocation algorithm was designed. The operational states for the energy resources were designed for coping with plugging and unplugging of energy resources on the fly (Section V-A). The task allocation algorithm was defined as a combination of three different

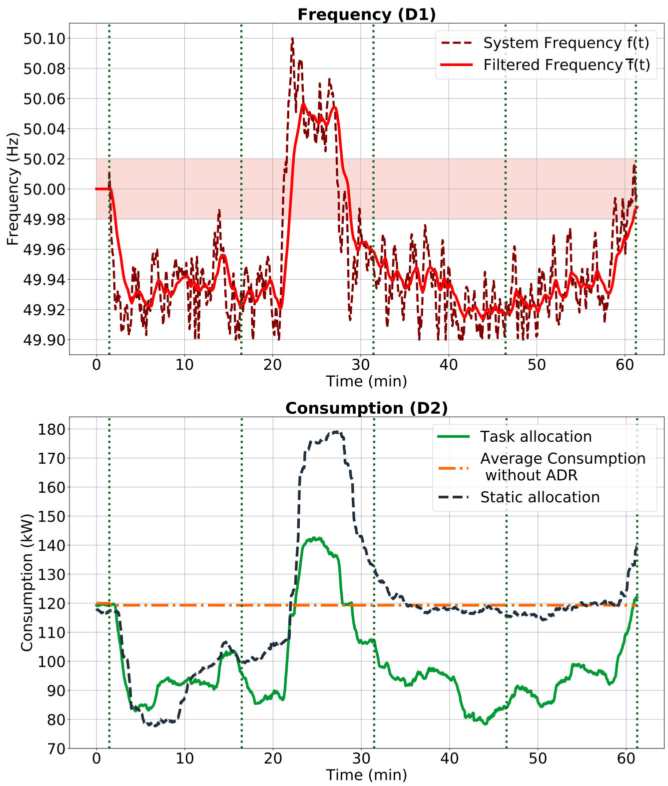

Fig. 10. (D1) The frequency $f(t)$ injected to the ADR system using real frequency data from Fingrid [50], and the filtered frequency $\overline{f}(t)$. (D2) The comparison of the provided reserve of the ADR system based on the task allocation with the static allocation of energy resources presented in [11].

procedures (Section V-B), where a multi-task, multi-resource, and multi-unit auction-based mechanism was employed as core solution. Moreover, a decentralized control logic was introduced to enable the energy resources to provide the FCR-N reserves (Section V-C).

The task allocation algorithm was shown to handle the plugging and unplugging of the energy resources and, combined with the message-oriented middleware, to avoid the need for hard real-time communication messages. These plug and play capabilities are not available in the state of the art technology discussed in Section VII-B. Moreover, the reaction of the ADR system proved to satisfy the requirements imposed by the TSO for the provision of FCR-N reserves, even though it was shown that a possible restriction could be given by the physical limits of the energy resources rather than the limitations of the communication. Nevertheless, these limitations can be hindered by employing a greater heterogeneity of energy resources with different characteristics (e.g. reaction time, resting period).

References

[1] P. González, J. Villar, C. A. Díaz, and F. A. Campos, "Joint energy and reserve markets: Current implementations and modeling trends," *Electric Power Systems Research*, vol. 109, pp. 101–111, 2014.

[2] P. Palensky and D. Dietrich, "Demand side management: Demand response, intelligent energy systems, and smart loads," *Industrial Informatics, IEEE Transactions on*, vol. 7, no. 3, pp. 381–388, 2011.

[3] M. H. Albadi and E. F. El-Saadany, "A summary of demand response in electricity markets," *Electric power systems research*, vol. 78, no. 11, pp. 1989–1996, 2008.

[4] ENTSO-E, "Supporting document for the network code on load-frequency control and reserves," 2015. [Online]. Available: https://goo.gl/txt3Xd

[5] NordREG, "Nordic market report 2014," 2014. [Online]. Available: https://goo.gl/a8FQoQ

[6] Y. G. Rebours, D. S. Kirschen, M. Trotignon, and S. Rossignol, "A survey of frequency and voltage control ancillary services - part i: Technical features," *IEEE Transactions on power systems*, vol. 22, no. 1, pp. 350–357, 2007.

[7] D. A. Halamay, T. K. A. Brekken, A. Simmons, and S. McArthur, "Reserve Requirement Impacts of Large-Scale Integration of Wind, Solar, and Ocean Wave Power Generation," *IEEE Transactions on Sustainable Energy*, vol. 2, no. 3, pp. 321–328, 2011.

[8] G. Lalor, A. Mullane, and M. O'Malley, "Frequency control and wind turbine technologies," *IEEE Transactions on Power Systems*, vol. 20, no. 4, pp. 1905–1913, nov 2005.

[9] J. A. Short, D. G. Infield, and L. L. Freris, "Stabilization of grid frequency through dynamic demand control," *IEEE Transactions on Power Systems*, vol. 22, no. 3, pp. 1284–1293, aug 2007.

[10] K. Samarakoon, J. Ekanayake, and N. Jenkins, "Investigation of domestic load control to provide primary frequency response using smart meters," *IEEE Transactions on Smart Grid*, vol. 3, no. 1, pp. 282–292, mar 2012.

[11] A. Molina-García, F. Bouffard, and D. S. Kirschen, "Decentralized demand-side contribution to primary frequency control," *Power Systems, IEEE Transactions on*, vol. 26, no. 1, pp. 411–419, 2011.

[12] S. A. Pourmousavi and M. H. Nehrir, "Real-time central demand response for primary frequency regulation in microgrids," *IEEE Transactions on Smart Grid*, vol. 3, no. 4, pp. 1988–1996, 2012.

[13] L. Gkatzikis, I. Koutsopoulos, and T. Salonidis, "The role of aggregators in smart grid demand response markets," *IEEE Journal on Selected Areas in Communications*, vol. 31, no. 7, pp. 1247–1257, 2013.

[14] C. Yuen, A. Oudalov, and A. Timbus, "The Provision of Frequency Control Reserves From Multiple Microgrids," *IEEE Transactions on Industrial Electronics*, vol. 58, no. 1, pp. 173–183, jan 2011.

[15] Fingrid, "Frequency containment reserves," 2018. [Online]. Available: https://goo.gl/aY2PSE

[16] C. Shao, X. Wang, X. Wang, C. Du, and B. Wang, "Hierarchical charge control of large populations of evs," *IEEE Transactions on Smart Grid*, vol. 7, no. 2, pp. 1147–1155, 2016.

[17] T. Chen, H. Pourbabak, Z. Liang, and W. Su, "An integrated evoucher mechanism for flexible loads in real-time retail electricity market," *IEEE Access*, vol. 5, pp. 2101–2110, 2017.

[18] J. A. Schachter and P. Mancarella, "Demand response contracts as real options: a probabilistic evaluation framework under short-term and long-term uncertainties," *IEEE Transactions on Smart Grid*, vol. 7, no. 2, pp. 868–878, 2016.

[19] K. Srikanth, L. Panwar, B. Panigrahi, R. Kumar, and Y. Hao, "Demand side management with consumer clusters in cyber-physical smart distribution system considering price based and reward based scheduling programs," *IET Cyber-Physical Systems: Theory & Applications*, 2017.

[20] A. Abiri-Jahromi and F. Bouffard, "Contingency-type reserve leveraged through aggregated thermostatically-controlled loads - part i: Characterization and control," *IEEE Transactions on Power Systems*, vol. 31, no. 3, pp. 1972–1980, 2016.

[21] Z. Ziadi, S. Taira, M. Oshiro, and T. Funabashi, "Optimal power scheduling for smart grids considering controllable loads and high penetration of photovoltaic generation," *IEEE Transactions on Smart Grid*, vol. 5, no. 5, pp. 2350–2359, 2014.

[22] I. Sharma, K. Bhattacharya, and C. Cañizares, "Smart distribution system operations with price-responsive and controllable loads," *IEEE Transactions on Smart Grid*, vol. 6, no. 2, pp. 795–807, 2015.

[23] Z. Akhtar, B. Chaudhuri, and S. Y. R. Hui, "Smart loads for voltage control in distribution networks," *IEEE Transactions on Smart Grid*, vol. 8, no. 2, pp. 937–946, 2017.

[24] V. C. Gungor, D. Sahin, T. Kocak, S. Ergut, C. Buccella, C. Cecati, and G. P. Hancke, "A survey on smart grid potential applications and communication requirements," *IEEE Transactions on Industrial Informatics*, vol. 9, no. 1, pp. 28–42, 2013.

[25] A. Zaballos, A. Vallejo, and J. M. Selga, "Heterogeneous communication architecture for the smart grid," *IEEE Network*, vol. 25, no. 5, pp. 30–37, 2011.

[26] R. de Diego, J.-F. Martínez, J. Rodríguez-Molina, and A. Cuerva, "A semantic middleware architecture focused on data and heterogeneity management within the smart grid," *Energies*, vol. 7, no. 9, pp. 5953–5994, 2014.

[27] L. Zhou and J. J. Rodrigues, "Service-oriented middleware for smart grid: Principle, infrastructure, and application," *IEEE Communications Magazine*, vol. 51, no. 1, pp. 84–89, 2013.
[28] Y. Jiang, "A survey of task allocation and load balancing in distributed systems," *IEEE Transactions on Parallel and Distributed Systems*, vol. 27, no. 2, pp. 585–599, 2016.
[29] P. Poullie, T. Bocek, and B. Stiller, "A survey of the state-of-the-art in fair multi-resource allocations for data centers," *IEEE Transactions on Network and Service Management*, 2017.
[30] Y. Zhang and M. Q. H. Meng, "Comparison of auction-based methods for task allocation problem in multi-robot systems," in *2013 IEEE International Conference on Robotics and Biomimetics (ROBIO)*, Dec 2013, pp. 2609–2613.
[31] M. Brambilla, E. Ferrante, M. Birattari, and M. Dorigo, "Swarm robotics: a review from the swarm engineering perspective," *Swarm Intelligence*, vol. 7, no. 1, pp. 1–41, 2013.
[32] O. Shehory and S. Kraus, "Methods for task allocation via agent coalition formation," *Artificial intelligence*, vol. 101, no. 1-2, pp. 165–200, 1998.
[33] J. Kalagnanam and D. C. Parkes, "Auctions, bidding and exchange design," in *Handbook of Quantitative Supply Chain Analysis*. Springer, 2004, pp. 143–212.
[34] C. Giovanelli, O. Kilkki, S. Sierla, I. Seilonen, and V. Vyatkin, "Towards a task allocation algorithm for frequency containment reserves," in *Industrial Informatics (INDIN), 2017 IEEE 15th International Conference on*. IEEE, 2017, pp. 765–768.
[35] A. Cornejo, A. Dornhaus, N. Lynch, and R. Nagpal, "Task allocation in ant colonies," in *International Symposium on Distributed Computing*. Springer, 2014, pp. 46–60.
[36] S. Parsons, J. A. Rodriguez-Aguilar, and M. Klein, "Auctions and bidding: A guide for computer scientists," *ACM Computing Surveys (CSUR)*, vol. 43, no. 2, p. 10, 2011.
[37] M. B. Dias, R. Zlot, N. Kalra, and A. Stentz, "Market-based multirobot coordination: A survey and analysis," *Proceedings of the IEEE*, vol. 94, no. 7, pp. 1257–1270, 2006.
[38] Y. Zhang, C. Lee, D. Niyato, and P. Wang, "Auction approaches for resource allocation in wireless systems: A survey," *IEEE Communications surveys & tutorials*, vol. 15, no. 3, pp. 1020–1041, 2013.
[39] S. Zaman and D. Grosu, "Combinatorial auction-based allocation of virtual machine instances in clouds," *Journal of Parallel and Distributed Computing*, vol. 73, no. 4, pp. 495–508, 2013.
[40] Mainsfrequency, "Measuring devices for frequency measurement," 2018. [Online]. Available: http://www.mainsfrequency.com/meter.htm
[41] Fingrid, "Application instruction for the maintenance of frequency controlled reserves," 2018. [Online]. Available: https://goo.gl/JkKZHf
[42] ENTSO-E, "Technical requirements for frequency containment reserve provision in the nordic synchronous area," 2017. [Online]. Available: https://goo.gl/5Pz4Zw
[43] C. Giovanelli, O. Kikki, A. Alahäivälä, I. Seilonen, M. Lehtonen, and V. Vyatkin, "A distributed ict architecture for continuous frequency control," in *6th International Conference on Smart Cities and Green ICT Systems, SMARTGREENS 2017, Porto, Portugal, 22-24 April 2017*, 2017, pp. 135–142.
[44] M. Stadler, W. Krause, M. Sonnenschein, and U. Vogel, "Modelling and evaluation of control schemes for enhancing load shift of electricity demand for cooling devices," *Environmental Modelling & Software*, vol. 24, no. 2, pp. 285–295, 2009.
[45] I. Pivotal Software, "Rabbitmq," 2017. [Online]. Available: https://www.rabbitmq.com/
[46] O. for the Advancement of Structured Information Standards (OASIS), "AMQP advanced message queuing protocol," 2017. [Online]. Available: https://www.amqp.org/
[47] J. E. Luzuriaga, M. Perez, P. Boronat, J. C. Cano, C. Calafate, and P. Manzoni, "A comparative evaluation of AMQP and MQTT protocols over unstable and mobile networks," in *2015 12th Annual IEEE Consumer Communications and Networking Conference (CCNC)*. IEEE, 2015, pp. 931–936.
[48] V. Kounev and D. Tipper, "Advanced metering and demand response communication performance in Zigbee based hans," in *Computer Communications Workshops (INFOCOM WKSHPS), 2013 IEEE Conference on*. IEEE, 2013, pp. 31–36.
[49] RabbitMQ, "Rabbitmq delayed message plugin," 2017. [Online]. Available: https://github.com/rabbitmq/rabbitmq-delayed-message-exchange
[50] Fingrid, "Frequency measurement data," 2018. [Online]. Available: https://goo.gl/c5Rrz9
[51] Mainsfrequency, "Continental europe frequency data," 2018. [Online]. Available: http://www.mainsfrequency.com/services.htm

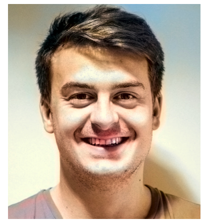

Christian Giovanelli received the M.Sc degree in Computer Engineering Information Technology and Smart Systems in 2014, from the Università degli Studi di Brescia, Brescia, Italy. Since 2015, he has been a Doctoral Candidate in the group of Information Technologies in Industrial Automation at Aalto University, Espoo, Finland. His main research interests include applying information technologies and artificial intelligence in the smart grid.

Olli Kilkki received his M.Sc degree from the Aalto University School of Electrical Engineering (formerly known as Helsinki University of Technology) in 2013, where he is a Doctoral candidate. His research interests include optimization, modeling and simulating control and information architectures in the smart grid.

Seppo Sierla (born 1977) received the Master of Science in Technology from Helsinki University of Technology with the major embedded systems in 2003. He received he degree of Doctor of Science in Technology from Helsinki University of Technology in 2007. He received the title of Docent at Aalto University School of Electrical Engineering in 2013 in the field "Software Design for Industrial Automation". Since 2011, he is a University lecturer at Aalto University, Finland. From 2003 to 2011 he was a Research scientist at Aalto University and Helsinki University of Technology. Before that he worked as a research assistant and as a software developer in two companies. He has 35 publications in Web of Science and holds one patent. His research interests include 3D simulation and virtualisation in the manufacturing and process industries. Dr. Sierla is a member of IEEE Industrial Electronics Society (IES) TC Industrial Informatics. He has been a track program committee member in 6 IES conferences. In 2016 he received a Recognition Award as responsible teacher for the course "Automation 1" at Aalto University School of Electrical Engineering.

Ilkka Seilonen received the Dr.Tech. degree in automation and systems engineering from the Helsinki University of Technology in 2006. He is currently a Senior Researcher with Aalto University. His research interest is in applying new information technologies to industrial applications.

Valeriy Vyatkin (M'03,SM'04) received Ph.D. degree from the State University of Radio Engineering, Taganrog, Russia, in 1992. He is on joint appointment as Chaired Professor of Dependable Computation and Communication Systems, Luleå University of Technology, Luleå, Sweden, and Professor of Information and Computer Engineering in Automation at Aalto University, Helsinki, Finland. He is also co-director of the international research laboratory of Computer Technologies at ITMO University, St. Petersburg, Russia. Previously, he was a Visiting Scholar at Cambridge University, U.K., and had permanent academic appointments with the University of Auckland, Auckland, New Zealand; Martin Luther University of Halle-Wittenberg, Halle, Germany, as well as in Japan and Russia. His research interests include dependable distributed automation and industrial informatics; software engineering for industrial automation systems; and distributed architectures and multi-agent systems applied in various industry sectors, including smart grid, material handling, building management systems, and reconfigurable manufacturing. Dr. Vyatkin was awarded the Andrew P. Sage Award for the best IEEE Transactions paper in 2012.